

# Quality control by a mobile molecular workshop: quality versus quantity

Ajeet K. Sharma<sup>1</sup> and Debashish Chowdhury\*<sup>1</sup>

<sup>1</sup>*Department of Physics, Indian Institute of Technology, Kanpur 208016, India.*

Ribosome is a molecular machine that moves on a mRNA track while, simultaneously, polymerizing a protein using the mRNA also as the corresponding template. We introduce quantitative measures of its performance which characterize, for example, the speed and fidelity of the template-dictated polymerization. We also define two different measures of efficiency and strength of mechano-chemical coupling of this molecular machine. We calculate all these quantities analytically. Some of these quantities show apparently counterintuitive trends of variation with the quality of kinetic proofreading. We interpret the origin of these trends. We suggest new experiments for testing some of the ideas presented here.

PACS numbers: 87.16.Ad, 87.16.Nn, 87.10.Mn

For cyclic machines with *finite cycle time*, the *efficiency at maximum power output* is a suitable indicator of its performance [1–3]. For molecular motors, the *Stokes efficiency* [4, 5] is an alternative measure of performance. However, not all machines are designed for the sole purpose of performing mechanical work. In this letter we consider a class of machines whose main function is to synthesize a hetero-polymer, subunit by subunit, using another hetero-polymer as the corresponding template.

The conceptual framework that we develop here is generally applicable to all machines which drive template-dictated polymerization. But, for the sake of concreteness, we formulate the theory here for a specific machine, namely, the ribosome [6]; it polymerizes a protein using a messenger RNA (mRNA) as the corresponding template and the process is referred to as *translation* (of genetic message). The subunits of a mRNA are nucleotides whereas that of a protein are amino acids. The correct sequence amino acids to be selected by the ribosome is dictated by the corresponding sequence of the codons (triplets of nucleotides). The ribosome also uses the mRNA template as the track for its movement. In each step, the ribosome moves forward by one codon on its track and the protein gets elongated by one amino acid.

For a ribosome, the average speed  $V$  of polymerization of a protein and the fidelity  $\phi$  of translation, rather than efficiency and power output, are the primary indicators of its performance. We define these quantities, as well as a few others, quantitatively and calculate these analytically.

A ribosome consists of two interconnected parts called the large and the small subunits. The small subunit binds with the mRNA track and decodes the genetic message of the codon whereas the polymerization of the protein takes place in the large subunit. The operations of the two subunits are coordinated by a class of adapter molecules, called tRNA. One end of a tRNA helps in the decoding process by matching its anti-codon with the codon on the mRNA while its other end carries an

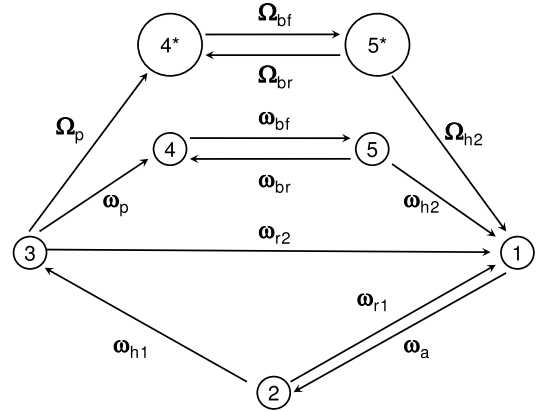


FIG. 1: Pictorial depiction of the full chemo-mechanical cycle of a single ribosome (see the text for details).

amino acid subunit; in this form the complex is called an amino-acyl tRNA (aa-tRNA).

The three main steps of each cycle of a ribosome are as follows: (i) selection of the cognate aa-tRNA, (ii) formation of the peptide bond between the amino acid brought in by the selected aa-tRNA and the elongating protein, (iii) translocation of the ribosome by one codon. However, some of these steps consist of important sub-steps. Moreover, the branching of paths from a well defined mechano-chemical state can give rise to the possibility of more than one cyclic pathway for a ribosome in a given cycle. Neither of these features were captured by the earlier models [7, 8]. The complete set of states and the pathways for a single ribosome in *our model* is shown in fig.1. This model may be regarded as an extension of the Fisher-Kolomeisky generic model for molecular motors [9].

The selection of aa-tRNA actually consists of two sub-steps. In the first sub-step, among the tRNAs, which arrive at the rate  $\omega_a$ , non-cognate ones are rejected, at the rate  $\omega_{r1}$ , because of codon-anticodon mismatch. The second sub-step implements a kinetic proofreading mechanism for screening out the near-cognate tRNAs; this sub-step is irreversible and involves hydrolysis of a GTP

\*Corresponding author(E-mail: debch@iitk.ac.in)

molecule (at the rate  $\omega_{h1}$ ). Near-cognate tRNAs are rejected at the rate  $\omega_{r2}$ . But, if the tRNA is cognate, the protein gets elongated by the addition of the corresponding amino acid (at the rate  $\omega_p$ ). However, occasionally a near-cognate tRNA escapes potential rejection and the ribosome erroneously incorporates it into the protein (at a rate  $\Omega_p$ ). The subsequent translocation step actually consists of important sub-steps. The first sub-step is a *reversible* relative (Brownian) rotation of the two sub-units with respect to each other (with rates  $\omega_{bf}$  and  $\omega_{br}$  along the correct path and with rates  $\Omega_{bf}$  and  $\Omega_{br}$  along the wrong path). In the state labelled by 4 (and 4\*), the tRNAs are in the so-called “hybrid” configuration [6] the details of which are not required for our purpose here. The second sub-step, which is *irreversible*, is driven by the hydrolysis of a GTP molecule; this sub-step leads to the coordinated movement of the tRNAs within the ribosome and the forward stepping of the ribosome by one codon on its mRNA track (at the rates  $\omega_{h2}$  and  $\Omega_{h2}$  along the correct and wrong paths, respectively). Further detailed identification of the states labelled in fig.1 by the integers [10] is not needed for our purpose here.

Thus, following selection of a cognate aa-tRNA, the correct pathway is  $1 \rightarrow 2 \rightarrow 3 \rightarrow 4 \rightarrow 5 \rightarrow 1$ . In contrast, if a non-cognate aa-tRNA is picked up, the most probable pathway is  $1 \rightarrow 2 \rightarrow 1$ . However, if the aa-tRNA is near cognate, then the pathway could be either  $1 \rightarrow 2 \rightarrow 3 \rightarrow 1$  (successful kinetic proofreading) or  $1 \rightarrow 2 \rightarrow 3 \rightarrow 4^* \rightarrow 5^* \rightarrow 1$  (incorporation of a wrong amino acid).

In principle, the model does not necessarily require any relation among the rate constants. However, throughout this letter we assume that

$$\omega_{r2} + \Omega_p = C, \quad (1)$$

a constant, because the more stringent the proofreading is, the fewer will be the wrong proteins produced.

We define the fraction

$$\phi = \frac{\omega_p}{\omega_p + \Omega_p} \quad (2)$$

as a measure of translational *fidelity*. The *error ratio*  $\epsilon = \Omega_p/(\omega_p + \Omega_p) = 1 - \phi$ , is the fraction of wrong amino acids incorporated in a protein. We also define the *rejection factor* as

$$\mathcal{R} = \left( \frac{\omega_{r1}}{\omega_{r1} + \omega_{h1}} \right) \left( \frac{\omega_{r2}}{\omega_{r2} + \omega_p + \Omega_p} \right). \quad (3)$$

The parameter  $\phi$  characterizes the “quality” of the final product while  $\mathcal{R}$  characterizes the “effort” of the quality control system in screening out the non-cognate tRNA (including near-cognate tRNA).

Suppose  $\mathcal{P}_\mu(t)$  is the probability of finding the ribosome in the “chemical” state  $\mu$  at time  $t$ , irrespective of its position on the mRNA track. The obvious normalization condition is  $\sum_{\mu=1}^5 \mathcal{P}_\mu + \mathcal{P}_4^* + \mathcal{P}_5^* = 1$ . Solving the master equations for  $\mathcal{P}_\mu(t)$ , written under mean-field

approximation, in the steady-state we get the average velocity

$$V = \ell_c(\omega_{h2}\mathcal{P}_5 + \Omega_{h2}\mathcal{P}_5^*) = \ell_c K_{eff} \left( 1 + \frac{\Omega_p}{\omega_p} \right) \quad (4)$$

where  $\ell_c$  is the length of a codon and

$$\begin{aligned} \frac{1}{K_{eff}} &= \frac{1}{\omega_a} \left( 1 + \frac{\omega_{r1}}{\omega_{h1}} \right) \left( 1 + \frac{\omega_{r2}}{\omega_p} \right) + \frac{1}{\omega_{h1}} \left( 1 + \frac{\omega_{r2}}{\omega_p} \right) \\ &+ \frac{1}{\omega_p} + \frac{1}{\omega_{bf}} \left( 1 + \frac{\omega_{br}}{\omega_{h2}} \right) + \frac{1}{\omega_{h2}} \\ &+ \left( \frac{\Omega_p}{\omega_p} \right) \left[ \frac{1}{\omega_a} \left( 1 + \frac{\omega_{r1}}{\omega_{h1}} \right) + \frac{1}{\omega_{h1}} \right. \\ &\quad \left. + \frac{1}{\Omega_{bf}} \left( 1 + \frac{\Omega_{br}}{\Omega_{h2}} \right) + \frac{1}{\Omega_{h2}} \right] \end{aligned} \quad (5)$$

Note that  $V$  is also identical to the average rate of elongation of the protein. Thus, in the special case  $\Omega_p = 0$ , different terms of  $K_{eff}^{-1}$  are the average time spent by the ribosome in different mechano-chemical states.

The direct transition  $3 \rightarrow 1$  gives rise to “slippage” [11]. Therefore, the coupling between the chemical input and the mechanical output is “loose” [12]. The ratio of the mechanical flux to chemical flux [13] can be taken as a measure of the strength of the mechano-chemical coupling  $\kappa$ :

$$\kappa = \frac{2(P_5\omega_{h2} + P_5^*\Omega_{h2})}{P_2\omega_{h1} + P_5\omega_{h2} + P_5^*\Omega_{h2}} \quad (6)$$

so that  $\kappa = 1$  in the limit  $\omega_{r2} = 0$ . Similar quantitative measures of mechano-chemical coupling has been introduced earlier [14] in the general context of motors which can execute “futile” cycles of hydrolysis of nucleotide triphosphates (including GTP). In the steady state of our model,

$$\kappa = \frac{2(\omega_p + \Omega_p)}{2(\omega_p + \Omega_p) + \omega_{r2}} = \frac{2(\omega_p + C - \omega_{r2})}{2(\omega_p + C) - \omega_{r2}} \quad (7)$$

Input power consumed in proofreading is

$$P_{in}^p = \left[ \left( \frac{\omega_{r2}}{\omega_{r2} + \omega_p + \Omega_p} \right) \omega_{h1} P_2 \right] \Delta\mu \quad (8)$$

whereas the input power consumed in protein synthesis

$$P_{in}^s = \left[ \left( \frac{\Omega_p + \omega_p}{\omega_{r2} + \Omega_p + \omega_p} \right) \omega_{h1} \mathcal{P}_2 + \Omega_{h2} \mathcal{P}_5^* + \omega_{h2} \mathcal{P}_5 \right] \Delta\mu \quad (9)$$

where  $\Delta\mu$  is the free energy released by the hydrolysis of a single GTP molecule. Thus, the total power input is

$$P_{in} = \left( \frac{\omega_{r2} + 2\omega_p + 2\Omega_p}{\omega_p} \right) K_{eff} \Delta\mu \quad (10)$$

We define the thermodynamic efficiency  $\eta_T$  and the Stokes efficiency  $\eta_S$  by the relations

$$\eta_T = \frac{FV}{P_{in}}, \quad \text{and} \quad \eta_S = \frac{\gamma V^2}{P_{in}} \quad (11)$$

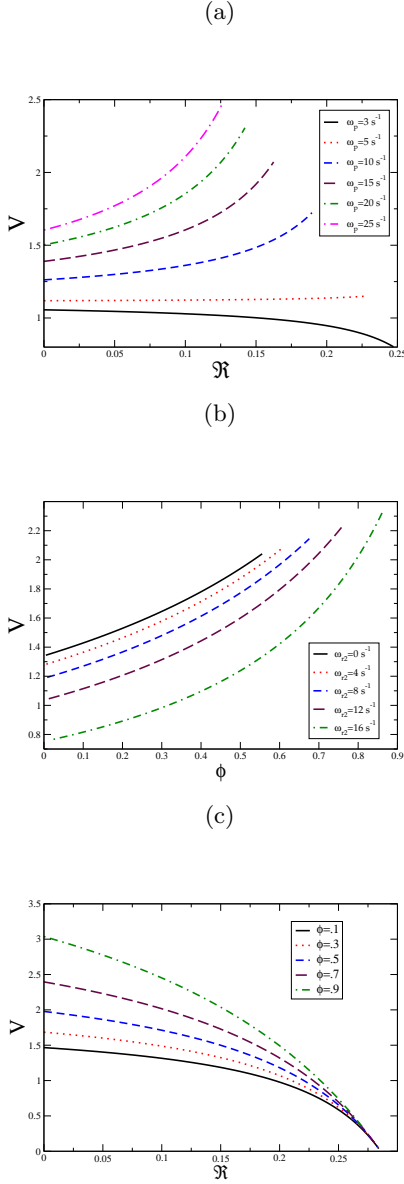


FIG. 2: The average velocity  $V$  of a ribosome (i.e., average rate of elongation of a protein) is plotted against (a) the rejection factor  $\mathcal{R}$ , (for six different fixed values of the parameter  $\omega_p$ ), (b) the fidelity  $\phi$  (for five different fixed values of the parameter  $\omega_{r2}$ ), and (c) the rejection factor  $\mathcal{R}$  (for five different fixed values of the fidelity  $\phi$ ).

where  $F$  is the load force and  $\gamma V$  is the phenomenological form of the viscous drag on the ribosome. Thus,  $\eta_S = (\gamma V/F)\eta_T$  and, using the expression (4) for  $V$ , we get

$$\eta_T = \frac{F\ell_c(\Omega_p + \omega_p)}{(\omega_{r2} + 2\omega_p + 2\Omega_p)\Delta\mu} \quad (12)$$

Moreover, we assume the standard form [9]

$$\omega_{h2}(F) = \omega_{h2}(0)\exp\left(-\delta\frac{F\ell_c}{k_B T}\right) \quad (13)$$

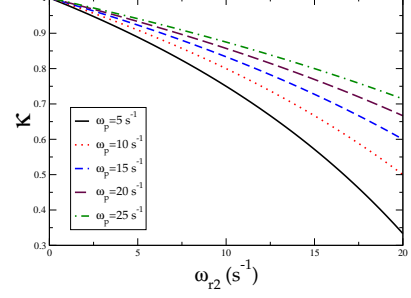


FIG. 3: The mechano-chemical coupling strength  $\kappa$  is plotted against  $\omega_{r2}$  for five different fixed values of the parameter  $\omega_p$ .

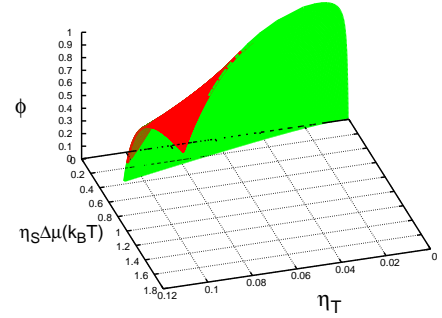


FIG. 4: Thermodynamic efficiency  $\eta_T$  and Stokes efficiency  $\eta_S$  are plotted against the fidelity  $\phi$ .

for the dependence of the mechanical translocation rate on the load force  $F$ . For plotting the graphs, we have used the parameter values  $F = 1\text{pN}$ ,  $\Delta\mu = 10k_B T$ ,  $\ell_c = 0.9\text{nm}$ ,  $\delta = 0.5$ ,  $\omega_a = 25.0$ ,  $\omega_{h1}(0) = \omega_{h2}(0) = 25.0$ ,  $\omega_{br} = \omega_{bf} = 10.0$ ,  $\omega_p = 25.0$ ,  $\gamma = 1.0$ . The parameters  $\omega_{r1}$  and  $\omega_{r2}$  have been varied over a wide range always keeping  $\omega_{r2} + \Omega_p = 20$ .

#### • Effects of kinetic proofreading and fidelity

The average rate  $V$  of elongation of a protein is plotted against the rejection factor  $\mathcal{R}$  and fidelity  $\phi$  in figs.2(a) and (b), respectively. Increase of  $\omega_{r2}$  increases the rejection factor  $\mathcal{R}$ . Therefore, naively, one would expect  $V$  to decrease with increasing  $\mathcal{R}$ . However, because of the constraint (1), increase of  $\omega_{r2}$  is compensated by decreasing  $\Omega_p$ . Therefore, instead of decreasing,  $V$  can increase with  $\mathcal{R}$  provided  $\omega_p$  is sufficiently large (see fig.2(a)).

Moreover, contrary to naive expectation,  $V$  increases with increasing  $\phi$  as long as  $\omega_{r2}$  is kept fixed (see fig.2(b)). However, for a given  $\phi$ ,  $V$  decreases with increasing  $\omega_{r2}$ ; this decrease is caused by the increasing frequency of the futile cycles in which a molecule of GTP is hydrolyzed in kinetic proofreading and the aa-tRNA is rejected. In order to emphasize the interplay of  $\mathcal{R}$  and  $\phi$  directly, in fig.??(c), we plot  $V$  against  $\mathcal{R}$  for several different values

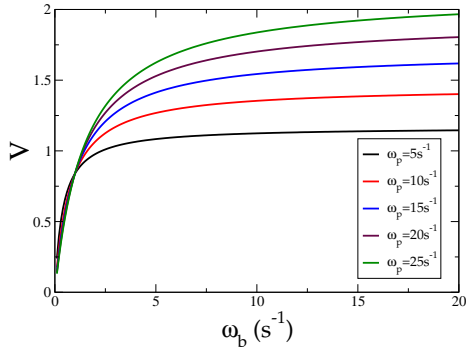


FIG. 5: The average velocity  $V$  of a ribosome (i.e., average speed of elongation of a protein) is plotted against  $\omega_b$ .

of the parameter  $\phi$ . Clearly, for a given  $\phi$ ,  $V$  decreases monotonically with  $\mathcal{R}$ . Similar monotonic decrease of  $V$  with increasing  $\omega_{r,2}$  demonstrates that the “slippage” caused by the kinetic proofreading weakens the mechano-chemical coupling  $\kappa$  (see fig.3).

The variation of the efficiencies  $\eta_T$  and  $\eta_S$  with  $\phi$  is shown in the 3-dimensional plot of Fig.4. Taking cross sections of this diagram parallel to the  $\eta_T - \eta_S$  plane for several different constant values of  $\phi$  (not shown in any figure) we find that  $\eta_T$  increases monotonically with  $\eta_S$ , but the increase is sublinear. This is a consequence of the fact that although  $\phi$  depends only on the ratio  $\Omega_p/\omega_p$ ,  $V$  depends separately also on  $\omega_p$  through its dependence on  $K_{eff}$ .

• *Effects of crosslinking the subunits*

By crosslinking the two subunits, Horan and Noller [15] demonstrated that, by preventing the Brownian rotation

of the two subunits relative to each other, protein synthesis can be stopped. Fig.5 shows the effect of varying the coupling strength of the crosslinks between the large and small subunits. It is well known that the entropic elasticity of a linear polymer decreases with increasing length. Therefore, The qualitative trend shown in fig.5 can be tested by repeating Horan and Noller’s experiment with crosslinks of several different lengths.

Intracellular machines which carry out template-dictated polymerization of macromolecules can be regarded as molecular motors [6, 16]. In this letter we have evaluated the performance of these machines in terms of *fidelity* and rate of polymerization, rather than efficiency and power output. The performance of all the intracellular machines of template-dictated polymerization can be characterized and evaluated within the general conceptual framework developed here. However, the results for polymerases [17], which polymerize DNA and RNA, would differ from those of ribosomes because of the differences between their respective mechano-chemical cycles. Using our theoretical model for a ribosome, we have analyzed the interplay of the “futile cycles” arising from kinetic proofreading and the consequent “looseness” of the mechano-chemical coupling. In contrast to the widespread belief, we show that a higher rate of polymerization of a protein does not necessarily compromise the translational fidelity. Moreover, we have predicted a monotonic decrease of the rate of protein polymerization with the increase of the elastic stiffness of the crosslinks between the large and small subunits of a ribosome. We have also suggested a possible experimental strategy to test this prediction.

We thank Joachim Frank for constructive criticism of an earlier draft of the manuscript.

- 
- [1] F.L. Curzon and B. Ahlborn, Amer. J. Phys. **43**, 22 (1975).  
[2] C. Van den Broeck, Phys. Rev. Lett. **95**, 190602 (2005).  
[3] T. Schmiedl and U. Seifert, EPL **81**, 20003 (2008).  
[4] H. Wang and G. Oster, Europhys. Lett. **57**, 134 (2002).  
[5] I. Derenyi, M. Bier and R. D. Astumian, Phys. Rev. Lett. **83**, 903 (1999).  
[6] J. Frank and R. L. Gonzales, Annu. Rev. Biochem. (2010) (in press).  
[7] A. Basu and D. Chowdhury, Phys. Rev. E **75**, 021902 (2007).  
[8] L. Ciandrini, I. Stansfield and M. C. Romano, Phys. Rev. E **81**, 051904 (2010).  
[9] A. B. Kolomeisky and M. E. Fisher, Annu. Rev. Phys. Chem. **58**, 675 (2007).  
[10] A. K. Sharma and D. Chowdhury (2010) to be published.  
[11] T. L. Hill, *Free energy transduction and biochemical cycle kinetics* (Dover, 2005).  
[12] F. Oosawa, Genes to cells **5**, 9 (2000).  
[13] Since  $\omega_{h,2}$  (and, similarly,  $\Omega_{h,2}$ ) accounts for a transition that is both “chemical” (hydrolysis of a GTP molecule) and “mechanical” (forward translocation) in nature, the corresponding flux appears both in the numerator and denominator of equation (6) defining  $\kappa$ .  
[14] M. Gyimesi, K. Sarlós, I. Derényi and M. Kovács, Nucleic Acids Res. (2010).  
[15] L.H. Horan and H.F. Noller, PNAS **104**, 4881 (2007).  
[16] J. Gelles and R. Landick, Cell **93**, 13 (1998).  
[17] N. Korzheva and A. Mustaev, in: *Molecular Motors*, ed. M. Schliwa (Wiley-VCH, 2003).